



In vitro and in vivo evaluation of an intraocular implant for glaucoma treatment

Mădălina V. Natu^a, Manuel N. Gaspar^b, Carlos A. Fontes Ribeiro^b, António M. Cabrita^c,
Hermínio C. de Sousa^a, M.H. Gil^{a,*}

^a Department of Chemical Engineering, University of Coimbra, Pólo II, 3030-790 Coimbra, Portugal

^b Institute of Pharmacology and Experimental Therapeutics, University of Coimbra, Pólo III, 3000-354 Coimbra, Portugal

^c Institute of Experimental Pathology, University of Coimbra, Pólo I, 3004-504 Coimbra, Portugal

ARTICLE INFO

Article history:

Received 8 April 2011

Received in revised form 17 May 2011

Accepted 18 May 2011

Available online 27 May 2011

Keywords:

Poly(ϵ -caprolactone)

Subconjunctival implant

Controlled drug release

In vivo

Intraocular pressure

Glaucoma

ABSTRACT

Implantable disks for glaucoma treatment were prepared by blending poly(ϵ -caprolactone), PCL, poly(ethylene oxide)-*b*-poly(propylene oxide)-*b*-poly(ethylene oxide) and dorzolamide. Their in vivo performance was assessed by their capacity to decrease intraocular pressure (IOP) in normotensive and hypertensive eyes. Drug mapping showed that release was complete from blend disks and the low molecular weight (MW) PCL after 1 month in vivo. The high MW PCL showed non-cumulative release rates above the therapeutic level during 3 months in vitro. In vivo, the fibrous capsule formation around the implant controls the drug release, working as a barrier membrane. Histologic analysis showed normal foreign body reaction response to the implants. In normotensive eyes, a 20% decrease in IOP obtained with the disks during 1 month was similar to Trusopt[®] eyedrops treatment. In hypertensive eyes, the most sustained decrease was shown by the high MW PCL (40% after 1 month, 30% after 2 months). It was shown that the implants can lower IOP in sustained manner in a rabbit glaucoma model.

© 2011 Elsevier B.V. All rights reserved.

1. Introduction

Glaucoma is a chronic condition that requires long-term treatment in order to stop progressive and irreversible blindness (Quigley, 2005). Treatment of glaucoma focuses on preserving vision by slowing down damage to the optic nerve. Therapy aims at preventing further damage by lowering IOP (or ocular hypertension) and it usually consists of pharmaceutical treatment and laser or surgical procedures (Schwartz and Budenz, 2004). It was shown that reducing IOP is effective in preventing disease progression in ocular hypertension, primary open angle glaucoma, and even in normal tension glaucoma (Khaw et al., 2004).

In most glaucoma patients, medical therapy consists of topical eyedrops and oral tablets. However, administration and compliance are often problematic. Eyedrops produce low ocular bioavailability (del Amo and Urtri, 2008), unnecessary systemic exposure (Korte et al., 2002) and have low patient compliance due to uncomfortable sensations (Noecker, 2005), as well as difficulty of instillation or forgetfulness (Kulkarni et al., 2008). Two main strategies have already been used clinically to diminish such effects, namely gel forming (viscous) solutions (Nanjawade et al., 2007) and controlled drug delivery systems (CDDS).

CDDS in the form of intraocular implants can deliver therapeutically effective amounts of drugs to targeted ocular tissues over sustained period of time without significant ocular/systemic side effects (Bourges et al., 2006). Thus, CDDS can be extremely suitable for chronic diseases, which require a constant level of medication to be maintained in the body over a long period of time. The major motivation for development and use of these devices is that they eliminate the need to take multiple doses of a drug during the day or week, thereby improving patient compliance and therapy outcomes (del Amo and Urtri, 2008).

In a previous work, implants based on poly(ϵ -caprolactone), PCL were prepared by solvent-casting, followed by dip-coating (Natu et al., 2011). Unfortunately, this preparation method is not reproducible and low drug loadings were achieved. High drug loads are needed for long term treatment of chronic diseases such as glaucoma. Moreover, the volume of such devices should be as small as possible in order to be easily introduced at the implantation site. Melt compression is a reproducible, easily scalable method of producing implants of different shapes and sizes (Yasukawa et al., 2005; Kuno and Fujii, 2010). In addition, compact implants can be obtained with small polymer-to-drug ratio, which enables high drug loads in a relatively small implant volume.

The objective of the present work was to prepare a drug loaded biodegradable implant designed to provide a localized, long-term (6 months to 2 years) sustained release of the drug, that can be used in the treatment of glaucoma. A subconjunctival placement of the

* Corresponding author. Tel.: +351 239798700; fax: +351 239798703.
E-mail address: hgil@eq.uc.pt (M.H. Gil).

implant is simple to perform because of easy access to the implantation area and low vascularization. PCL and Lutrol F 127, Lu were selected because they are both biocompatible, biodegradable and they can be easily processed by conventional polymer processing techniques (Breitenbach, 2002). Moreover, they are commercially available, inexpensive and well characterized polymers. PCL is a slowly degradable polymer, while Lu can be used as a release modulator (Natu et al., 2008; Natu et al., 2010). Two molecular weights of PCL were used because it was shown that molecular weight determines the time lag before erosion and the rate of bioerosion in vivo (Pitt et al., 1981). The implantable drug loaded disks were prepared by melt compression and their performance in vivo was evaluated by assessing the capacity to lower IOP in normotensive and hypertensive rabbit eyes.

2. Materials and methods

2.1. Preparation of polymer disks

Poly(ϵ -caprolactone) (PCL40, average M_w 65,000 g/mol and PCL10, average M_w 15,000 g/mol, Sigma–Aldrich) and Lutrol F 127 (Lu, poly(ethylene oxide)-b-poly(propylene oxide)-b-poly(ethylene oxide), 9000–14,000 g/mol, 70% by weight of polyoxyethylene, BASF) films and dorzolamide hydrochloride (Chemos GmbH) loaded films (Lu/PCL: 13/87, 6/94, 0/100%, w/w) were prepared by solvent casting from acetone (UV grade, Sigma–Aldrich) at 40 °C, using a 15% (w/v) total polymer concentration and 33.3% (w/w) theoretical drug loading. Polymer sheets were fabricated by compression moulding of the polymer films in a stainless steel mould by applying a pressure of 201.5 kg/m² for 20 min at 100 °C. The mould was subsequently cooled under a jet of cold water (20 °C) during 2 min. Discs of 4 mm diameter (1 mm thickness, 4–5 mg drug mass, 13–16 mg total mass) were punched from the polymer sheets. They were used as such in characterization tests. Prior to in vivo implantation, the discs were sterilized using UV radiation during 20 min (at 254 nm) in a UV chamber (Camag UV cabinet).

2.2. Disk characterization

Differential scanning calorimetry (DSC) was carried out using a DSC Q100 equipment (TA Instruments) under nitrogen atmosphere (100 ml/min). Samples with masses of approximately 5 mg were heated until 100 °C, at a heating rate of 10 °C/min. The relative crystallinity of the disks was calculated as previously described considering the melting enthalpy of 100% crystalline PCL and 100% crystalline Lu (Natu et al., 2010). Thermogravimetric analysis (TGA) was carried out using a SDT Q 600 equipment (TA Instruments). Samples with masses of approximately 10 mg were heated until 600 °C, at a heating rate of 10 °C/min. The degradation temperature (T_d) was determined at the onset point of the TGA plot.

Water contact angle was evaluated by static contact angle measurements using an OCA 20 Video-Based Contact Angle Meter (Dataphysics) and employing the sessile drop method.

Drug loading of the disks was assessed by elemental analysis (quantification of sulphur, present only in the drug molecule).

2.3. Morphology and drug distribution

The morphology of the disks (before and after implantation) was examined using scanning electron microscopy, SEM (JSM 5310, Jeol). The drug mapping (elemental sulphur) of the disks surface and cross-section (showing the center of the disk) was done using electron probe microanalysis, EPMA (Camebax SX50, Cameca) at 15 kV accelerated voltage and 40 nA probe current.

2.4. In vitro and in vivo degradation

The extent of hydrolytic degradation of the disks (as prepared, in vitro degraded and in vivo degraded) was evaluated by determining the change of MW in time. Polymer disks were placed in 4 ml PBS with 0.001% sodium azide, at 37 °C. The changes in the MW were measured by size exclusion chromatography (SEC), using chloroform as mobile phase (1 ml/min, 30 °C) and a PLgel MIXED-C column (300 mm × 7.5 mm, 5 μ m, Varian). PL-EMD 960 (Polymer Laboratories) evaporative light scattering detector was used to acquire the data. Universal calibration was performed using polystyrene (PS) standards and Mark–Houwink parameters $k_{PCL} = 1.09 \times 10^{-3}$ dl/g, $\alpha_{PCL} = 0.60$, $k_{PS} = 1.25 \times 10^{-4}$ dl/g, $\alpha_{PS} = 0.71$. Peak integration was performed using Clarity chromatography software (DataApex).

2.5. In vitro drug release and release modelling

Dorzolamide hydrochloride release was studied in 10 ml phosphate saline buffer medium (PBS tablets, pH 7.4, 10 mM phosphate, 137 mM sodium, 2.7 mM potassium, Sigma–Aldrich) at 37 °C. At scheduled time intervals, samples were taken and the entire medium volume was replaced with fresh medium to maintain sink conditions. The mass of dorzolamide hydrochloride released at time t was determined by UV spectroscopy at 254 nm (Jasco V-650 Spectrophotometer). The percentage of in vitro released drug was calculated using Eq. (1).

$$\text{Released drug in vitro (\%)} = \frac{M_{dt}}{M_{d0}} \times 100 \quad (1)$$

In Eq. (1), M_{dt} is the drug mass released at time t and M_{d0} is the initial drug mass.

In order to study the drug release mechanism, the power law equation (Eq. (2)) which is based on diffusional model of drug transport, was used, where M_t/M_{total} is the fractional release of the drug, k is the kinetic constant and n is the release exponent, indicating the mechanism of drug release (Natu et al., 2010).

$$\frac{M_t}{M_{total}} = kt^n \quad (2)$$

An alternative model (Eq. (3)) based on polymer degradation control of drug release was used to fit the release data. In this model, two pools of drug are considered: a pool of mobile drug which readily diffuses out of the matrix upon immersion in an aqueous medium and a pool of immobilized drug which can diffuse only after matrix degradation (Natu et al., 2010). This model can be applied to slow-degrading polymers such as PCL due to the fact that polymer degradation is much slower than drug diffusion and as such it is the rate limiting step for drug transport.

$$M(\tau) = A_0 + |\Omega|S_0(1 - \exp(-\tau)), \quad \bar{\alpha}_{lim}^{-1} \rightarrow 0 \quad (3)$$

In Eq. (3), A_0 is the load of the mobile drug, S_0 is the load of immobilized drug, τ is the dimensionless time and is defined by $\tau = \mu t$ (μ is the degradation rate constant) and Ω is the geometrical factor. The model parameters were determined by non-linear regression and the goodness of the fit was assessed.

2.6. Disk implantation, glaucoma model, intraocular pressure measurement and in vivo drug release

New Zealand white rabbits were used in animal experiments in agreement with European Union Council Directive 86/609/EEC regarding the protection of animals used for experimental and other scientific purposes as described before (Natu et al., 2011). The disk implantation procedure and the IOP measurement by tonometry were already described (Natu et al., 2011). In order to produce

Table 1
Water contact angle, melting and degradation temperatures of the disks.

Sample	T_d ($^{\circ}\text{C}$)	T_m ($^{\circ}\text{C}$)	Contact angle (deg)
PCL40 + drug	279.38, 420.20	61.53 (0.03)	80.23 (2.63)
PCL40	375.51	61.26 (0.31)	73.88 (3.31)
PCL10 + drug	275.00, 420.33	60.67 (0.19)	78.26 (1.24)
PCL10	269.62, 421.88	61.23 (0.61)	70.24 (1.86)
6%Lu,PCL40 + drug	–	61.45 (0.42)	46.87 (2.78)
6%Lu,PCL40	–	62.07 (0.17)	32.52 (2.12)
13%Lu,PCL40 + drug	–	58.22 (0.26)	39.88 (0.80)
13%Lu,PCL40	–	58.86 (0.45)	40.20 (2.53)
Lu	358.80	55.57 (0.65)	59.33 (0.35)

high IOP, we used a low temperature ophthalmic cautery (Bovie, Aaron Medical) to produce 30–50 burns that were directed at the limbal plexus and at the episcleral veins (Levkovitch-Verbin et al., 2002; Ruiz-Ederra and Verkman, 2006).

The animals were divided in three groups: group 1 ($n=26$) received drug loaded polymer disks (the right eye contained the drug loaded disk – PCL40, PCL10, 6%Lu,PCL40 and 13%Lu,PCL40, while the left had the control disk – polymers without drug), group 2 ($n=3$) was submitted to Trusopt[®] eyedrops (dorzolamide

hydrochloride 2%, Chibret) treatment (1 drop twice a day in the right eye, while the left eye received a drop of balanced salt solution, BSS sterile solution, Alcon), while group 3 ($n=3$) was the glaucoma model reference.

For in vivo release tests, previously weighed polymer disks were implanted as described before for predetermined periods of time and subsequently removed, cleaned of ocular tissues, rinsed with distilled water and vacuum-dried to constant weight. The in vivo released mass of drug was determined gravimetrically using Eq.

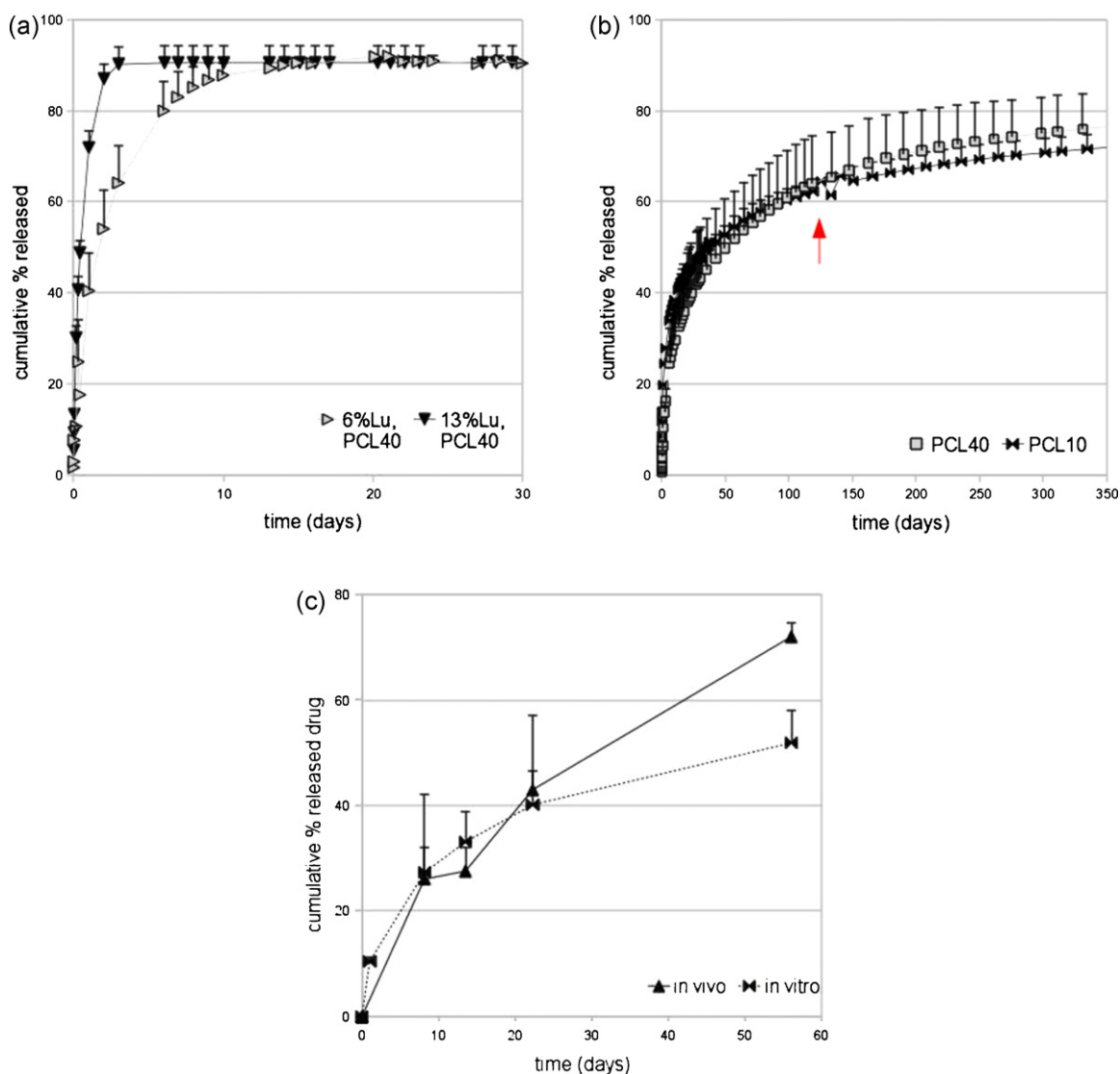


Fig. 1. (a and b) In vitro drug release (the red arrow indicates the point on the kinetics curve when the released dose is smaller than the effective dose) and (c) comparison between in vivo and in vitro drug release for sample PCL40. (For interpretation of the references to color in this figure legend, the reader is referred to the web version of this article.)

Table 2
Released drug percentages for in vitro tested disks and disks implanted during 1 month or 2 months.

Sample	In vitro		In vivo			
	Rel. drug (%)		Rel. drug mass (mg)		Rel. drug (%)	
	1 month	2 months	1 month	2 months	1 month	2 months
PCL40	40.14 (6.48)	51.88 (6.07)*	2.22 (0.72)	3.72 (0.13)	42.99 (14.06)	72.02 (2.49)*
PCL10	47.29 (0.96)*	–	4.47 (0.18)	–	83.30 (4.01)*	–
6%Lu,PCL40	90.98 (1.06)	–	4.74 (0.20)	–	96.80 (1.62)	–
13%Lu,PCL40	90.57 (3.79)	–	4.95	–	94.56	–

* $p \leq 0.1$ statistically significant differences between in vitro and in vivo drug released percentages.

Table 3
Model parameters determined by non-linear regression.

Sample	Power law			Degradation model			
	k (day ⁻ⁿ)	n	R^2_{adj}	A_0	S_0	μ (day ⁻¹)	R^2_{adj}
PCL40	17.05 (0.65)	0.26 (0.01)	0.98	10.75 (1.42)	62.21 (1.64)	0.02 (0.00)	0.96
PCL10	24.11 (0.60)	0.19 (0.01)	0.97	15.86 (1.67)	51.45 (1.86)	0.04 (0.00)	0.92
6%Lu,PCL40	41.31 (3.14)	0.27 (0.03)	0.92	5.90 (1.33)	84.12 (1.46)	0.42 (0.03)	0.99
13%Lu,PCL40	56.23 (3.53)	0.17 (0.02)	0.83	7.01 (0.66)	83.41 (0.69)	1.66 (0.04)	1.00

Table 4
Average IOP reduction.

Sample	Average IOP reduction (%)			
	Normotensive eyes		Hypertensive eyes	
	1 month	2 months	1 month	2 months
Trusopt	16.55 (10.94)	–	25.21 (9.74)	23.82 (10.14)
PCL40	16.91 (6.43)	–	41.06 (12.16)*	33.21 (8.90)
PCL10	23.73 (8.15)	–	39.61 (11.90)*	–
6%Lu,PCL40	23.85 (7.24)	–	39.24 (15.21)*	–
13%Lu,PCL40	16.59 (8.02)	–	–	–

* $p \leq 0.01$ statistically significant differences between IOP percentages obtained by disk implantation relative to those obtained with Trusopt instillation.

(4). In Eq. (4), M_i is the initial disk mass, M_t is the disk mass after implantation time t , M_c is the mass loss of the control disk and M_{d0} is the initial drug mass.

$$\text{Released drug in vivo (\%)} = \frac{M_i - M_t - M_c}{M_{d0}} \times 100 \quad (4)$$

In vivo drug released percentages were also determined by elemental analysis (the residual drug was determined after in vivo implantation).

2.7. Histologic evaluation

The local implant site and important organs were excised for histological evaluation. The collected organs included kidneys, spleen, liver, lung (only after 2 months implantation). The organs and tissue samples were fixed in 10% neutral buffered formaldehyde. The samples were then embedded in paraffin and dehydrated by isopropanol processing. Thin layers were cut from the samples with

a microtome and stained with hematoxylin and eosin for optical microscopy.

2.8. Statistics

All values are presented as mean and standard error of the mean (SEM). Experiments were performed in triplicates. Statistical analysis (Student's T -test, independent, two-tailed) was done using OpenOffice.org Calc 3.1.

3. Results and discussion

3.1. Disk characterization

In Table 1, melting (T_m) and degradation temperatures (T_d) are presented for drug loaded and control disks because their knowledge is required when dealing with polymer processing methods for the manufacture of drug-eluting implants. Blend disks are more

Table 5
Peak IOP and the time interval from instillation/implantation to peak IOP.

Sample	Peak IOP reduction (%)/time (days)			
	Normotensive eyes		Hypertensive eyes	
	1 month	2 months	1 month	2 months
Trusopt	27.85/0.96	–	36.59 (2.37)/3.38	35.33 (3.65)/34.56
PCL40	25.67/7.35	–	55.26 (0.98)/6.90	43.24 (2.55)/25.06
PCL10	35.92/6.90	–	50.21 (0.00)/6.94	–
6%Lu,PCL40	32.00/4.38	–	55.23 (5.03)/3.18	–
13%Lu,PCL40	29.96/2.42	–	–	–

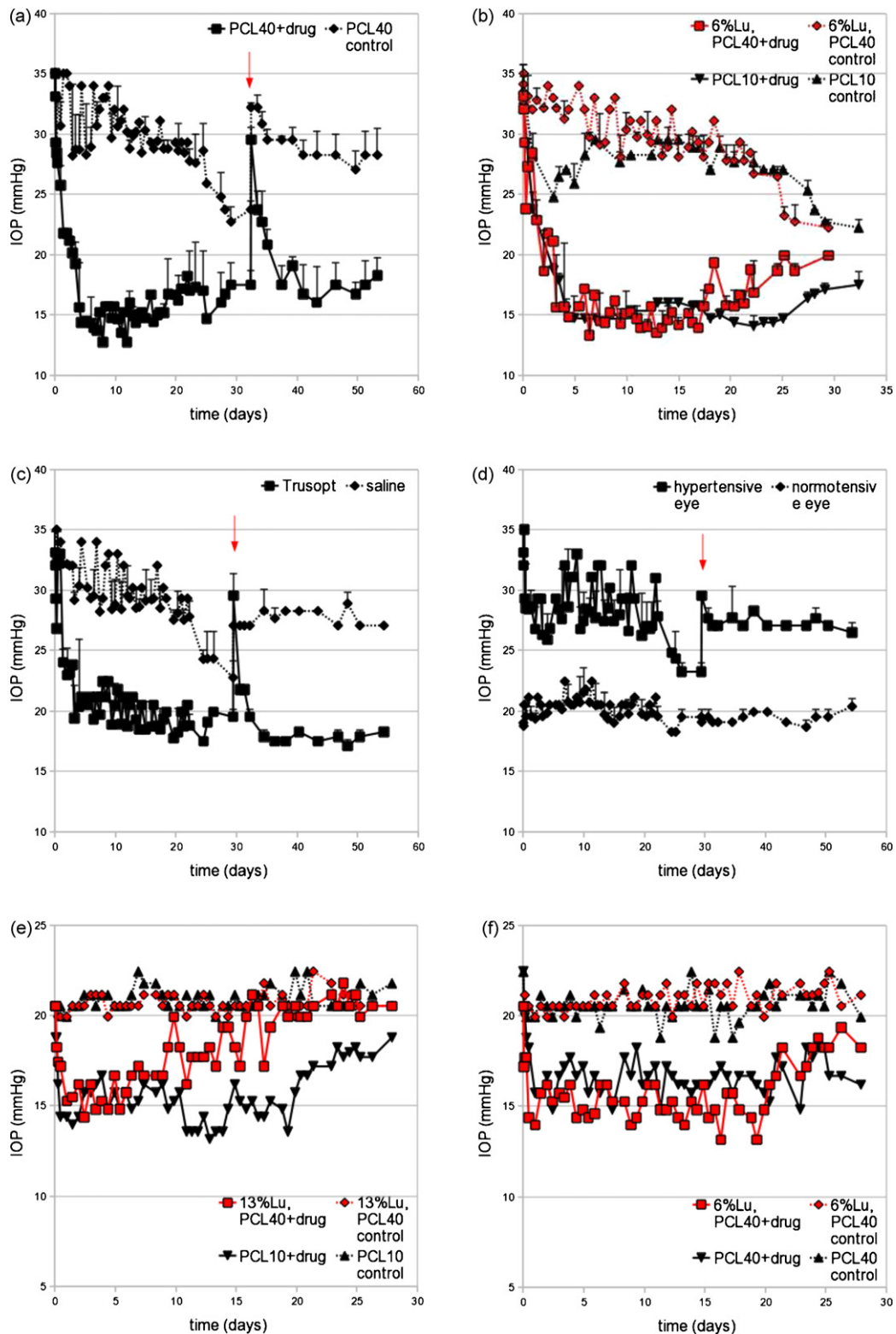


Fig. 2. (a and b) IOP in hypertensive eyes of group undergoing implant treatment, (c) IOP in hypertensive eyes of group undergoing Trusopt® eyedrops treatment, (d) IOP in glaucoma model group, (e and f) IOP in normotensive eyes of group undergoing implant treatment (the red arrow indicates the point when a second cauterization was performed). (For interpretation of the references to color in this figure legend, the reader is referred to the web version of this article.)

hydrophilic than PCL disks due to the incorporation of hydrophilic Lu (Natu et al., 2008; Natu et al., 2010) as shown by the lower contact angle values. The low T_m enables processing at temperatures much lower than the degradation temperature of dorzolamide ($T_d = 251.26^\circ\text{C}$). The PCL samples show a two step degradation pro-

cess, the first step corresponding to drug degradation, while the second corresponds to polymer degradation.

All disks presented an average content of sulphur of 33.6%, which corresponds to approximately 5 mg of loaded drug in each disk.

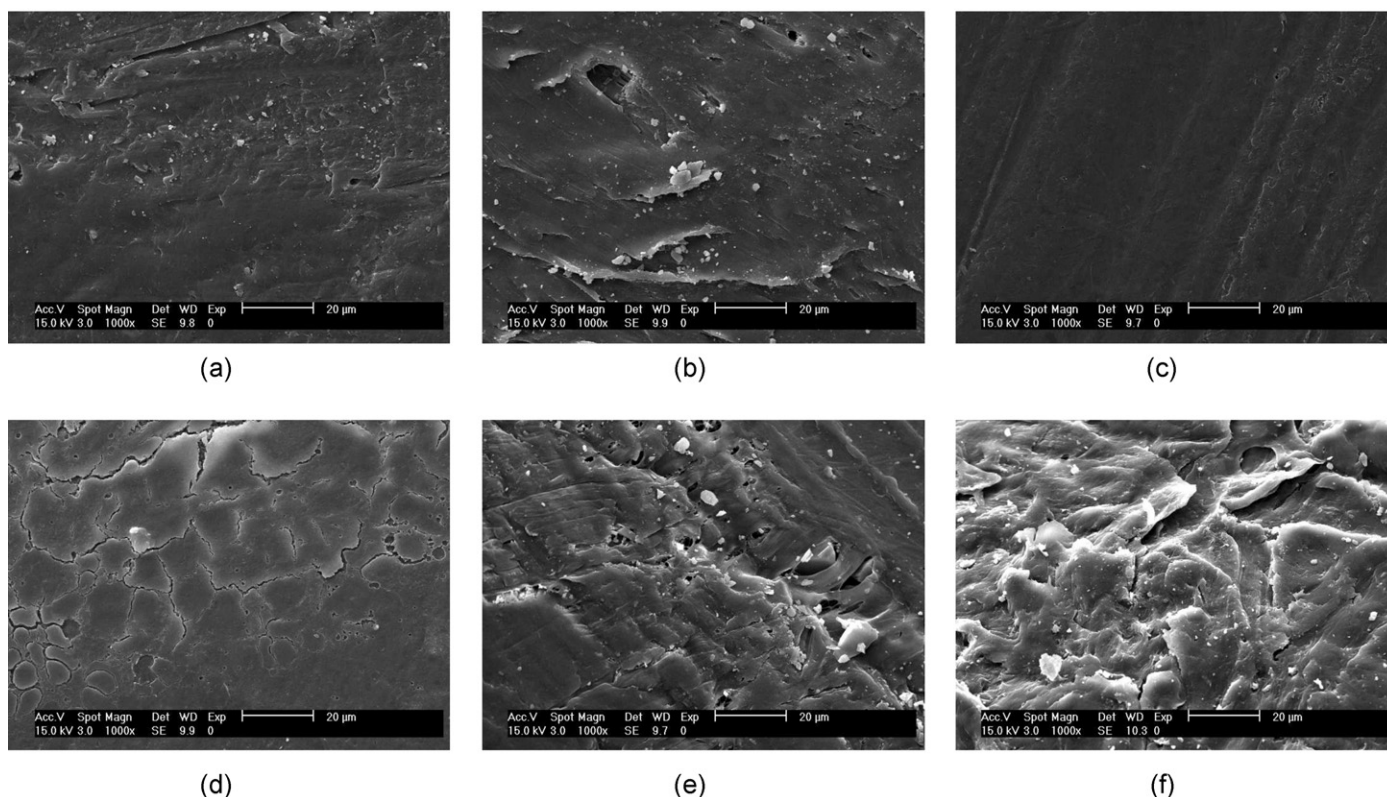


Fig. 3. SEM of disks (with drug) surface. (a) PCL40 as prepared, (b) PCL40 in vivo, (c) PCL10 as prepared, (d) PCL10 in vivo, (e) 6%Lu,PCL40 as prepared, and (f) 6%Lu,PCL40 in vivo.

3.2. General considerations about implantation surgical procedure and animal wellbeing

The surgical procedure to insert the disks is relatively easy to perform because of easy access to the implantation area and low vascularization. Moreover, the wound does not need to be sutured because a pocket is created that keeps the disk in place. The fixation of the disk is further enhanced by fast wound healing as the disk is completely encapsulated by the conjunctiva. Ocular adverse events included conjunctivitis (6 eyes in 64 eyes), that resolved clinically in less than 1 week (with antibiotic eyedrops). No other events were observed. It should be mentioned that such ocular adverse events (conjunctival hyperemia, stinging, burning, foreign body sensation, tearing, vision blurring) are quite frequent in topical treatment with eyedrops (Noecker, 2005).

3.3. In vitro and in vivo drug release

Each disk was loaded with approximately 5 mg of drug in order to achieve a release rate of 18 µg/day (similar with the one obtained with Trusopt® 2% instillation three times a day (Schmitz et al., 1999) for at least 4.5 months (we considered 50% drug losses during the transport from conjunctiva to ciliary body).

Fig. 1(a) presents the release from blends: release is almost complete after 10 days for 13%Lu,PCL40 and after 20 days for 6%Lu,PCL40. The release kinetics shown in Fig. 1(b) presents similar released drug percentages regardless of the PCL molecular weight.

A comparison between released drug percentages in vitro and in vivo is shown in Table 2. It can be noted that there are significant differences between released percentages in vitro and in vivo for PCL40 and PCL10 samples ($p = 0.07$ and $p = 0.01$, respectively), while the released drug percentages of 6%Lu,PCL40 and 13%Lu,PCL40 are similar in vitro and in vivo ($p = 0.15$ for 6%Lu,PCL40). In vivo

drug released percentages (calculated by mass balance) for PCL40 implant were confirmed by elemental analysis (the residual drug was determined after in vivo implantation): after 8 days, 22.69 (5.82)% released drug, after 14 days, 24.09 (2.93)% released drug and after 22 days, 35.74 (11.54)% released drug.

In vivo release kinetics (Fig. 1(c)) seems to approach a zero-order kinetics, while the in vitro kinetics curves (Fig. 1(b)) appear to have a $t^{0.5}$ profile. This may be due to different release controlling phenomena: in vitro, diffusion controls drug release (from here the classic, Fickian $t^{0.5}$ profile), while in vivo, the fibrous capsule formation around the implant (see Section 3.7) controls the drug release, functioning as a barrier membrane that slows down release. Thus, there should be significant differences between drug released in vitro and in vivo (see Table 2) for PCL40 and PCL10 samples. For blend samples, due to polymer erosion that takes place mostly in the first day of release (Natu et al., 2010), the fibrous capsule/barrier control is absent (only after 1 week, the disks were fully encapsulated) and as such the released drug percentages are similar both in vitro and in vivo.

In Table 3, the non-linear regression results are presented. The objective behind fitting these equations to the release data was to understand the underlying phenomena involved in the drug release mechanism. Smaller values for S_0 suggest higher amounts of immobilized drug that will not be released (37.8% for PCL40 and 16.6% for 13%Lu,PCL40). The percentage of immobilized drug is higher for PCL40 than for blend samples because in the latter case erosion creates more surface area and exposes more drug to water dissolution that otherwise would be trapped. In the case of the studied polymers, physical immobilization of the drug occurs due to drug entrapment in crystalline regions. Drug diffusion from these regions is hindered because water enters initially only in the amorphous parts. The immobilized fraction of the drug will be released only with polymer degradation (this explains why the steady state

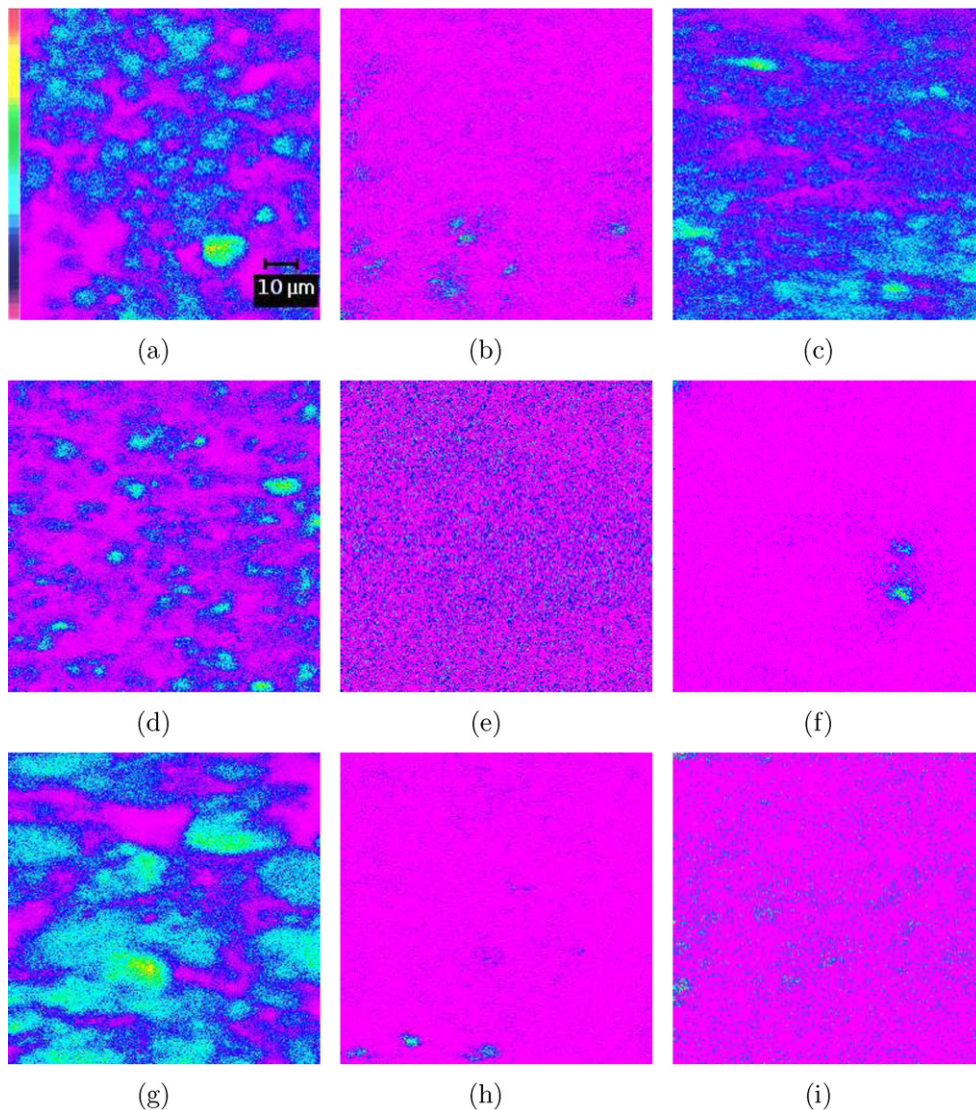


Fig. 4. Sulphur drug mapping after 1 month in vivo. (a) PCL40 surface as prepared, (b) PCL40 surface in vivo, (c) PCL40 section in vivo, (d) PCL10 surface as prepared, (e) PCL10 surface in vivo, (f) PCL10 section in vivo, (g) 6%Lu,PCL40 surface as prepared, (h) 6%Lu,PCL40 surface in vivo, (i) 6%Lu,PCL40 section in vivo (in the scale bar, the colour gradient represents 0% drug (pink) and 100% drug (red)). (For interpretation of the references to color in this figure legend, the reader is referred to the web version of this article.)

value of released drug percentage is smaller than 100%, which would correspond to total release).

The regression results obtained using power law equation reinforce the previous observations. The high value of k indicates the extent of burst, higher for blend samples. The range of values for the release exponent is indicative of a diffusion mechanism for drug release. This model fails to explain the last stage of the release (steady-state at less than 100% released drug) as it does not consider the effect of polymer degradation.

The release kinetics suggested a three stage release mechanism, with different steps depending on disk composition. Dissolution of the surface loaded drug and subsequent diffusion, followed by diffusion of the mobile drug through water-filled pores (created either due to Lu leaching or polymer recrystallization (Natu et al., 2010; Miyajima et al., 1997), while the last stage was controlled by polymer degradation and subsequent diffusion of the immobilized drug. In blends, most of the drug is released due to polymer erosion, while the residual drug was released by diffusion through water-filled pores. The mechanism from PCL40/PCL10 disks and blend disks is essentially the same, except for the initial stage when drug diffusion

is coupled with polymer erosion in the case of blends. By selecting the proper ratio between the components, the preponderance of a certain stage during drug release can be changed, obtaining an overall effect in drug release that fits the intended application.

3.4. Intraocular pressure measurement

In order to simulate ocular hypertension, we developed a rabbit glaucoma model by increasing the IOP values (Fig. 2(d)) from an average of 20.9 mmHg (normotensive eyes) to an average of 30.1 mmHg (hypertensive eyes). A second procedure was performed after 1 month because IOP values returned to baseline after this period (Levkovitch-Verbin et al., 2002; Ruiz-Ederra and Verkman, 2006). Disks were first tested in normotensive eyes in order to select the best performing systems. In Fig. 2(e) and (f), it can be seen that sample 13%Lu,PCL40 decreased IOP by 16.6% (see also Table 4) reaching the baseline value after 15 days, while sample 6%Lu,PCL40 decreased IOP by 23.8% during 25 days. More sustained decrease in IOP was shown by sample PCL40 (16.9%) and PCL10 (23.7%) during the 30 days of test. The decrease in IOP obtained

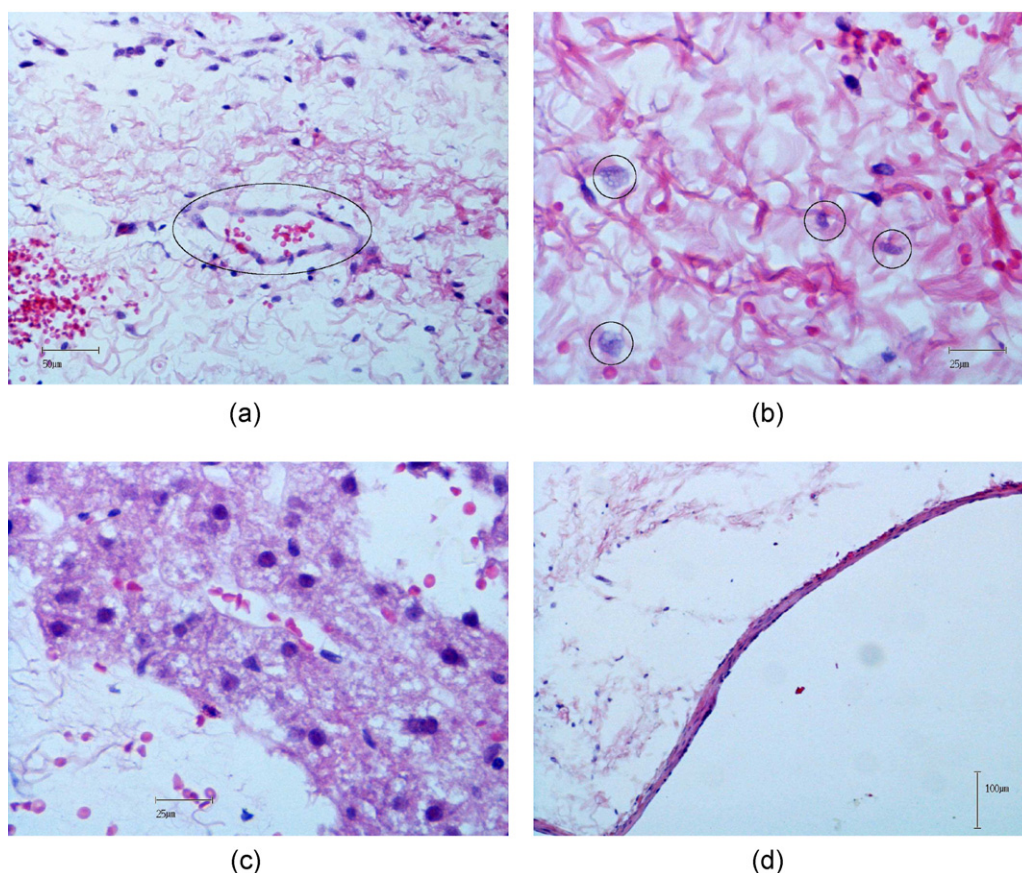


Fig. 5. Light microscopy images of implanted disk showing (a) cells and blood vessel (shown in the ellipse); (b) macrophage cells (highlighted by circles); (c) foreign-body giant cell; (d) fibrous capsule.

with the disks was comparable with the one obtained by applying Trusopt eyedrops ($p \geq 0.17$ for all disks). A decrease of at least 20% is desired in order to reduce the rate of open angle glaucoma-related damage (Yudcovitch, 2010).

Fig. 2(a) and (b) present IOP change in hypertensive eyes with implanted disks and in eyes treated with Trusopt® (Fig. 2(c)). PCL40 presented a decrease of 41.1% after 1 month and a decrease of 33.2% after 2 months, which is particularly suitable for patients with moderate to severe glaucoma (Yudcovitch, 2010). IOP values in eyes with PCL40 implants are expected to approach the baseline values after approximately 3 months (see Fig. 1(b)). Samples PCL10 and 6%Lu,PCL40 showed similar IOP decrease percentages and peak IOP percentage in hypertensive eyes, while peak IOP was attained faster for sample 6%Lu,PCL40 due to faster drug release (see Section 3.3). Thus, the release rate from the disks can be manipulated by blending in order to achieve the desired decrease in IOP.

Table 4 presents the average IOP decrease percentages achieved by the implanted disks in normotensive and hypertensive eyes, while Table 5 shows the peak IOP decrease and the time interval from instillation/implantation to peak IOP. It can be noted that there was a higher IOP decrease in hypertensive eyes than in normotensive eyes for eyedrops and disks ($p \leq 0.01$ for all disks). Sample PCL40 showed the best performance in vivo (constant decrease in IOP for longer time) due to more sustained drug release. The obtained values for IOP decrease with Trusopt® are in agreement with literature values for normotensive (Harris et al., 2000; Scozzafava et al., 1999) and hypertensive eyes (Konstas et al., 2008; Seki et al., 2005). There was a higher decrease in IOP for eyes treated with disks than in those treated with eyedrops ($p \leq 0.01$ for all disks) probably because of higher amounts of drug released by the disks

(average in vitro release rate of 0.43 (0.04) mg/day for PCL40 or 1.34 (0.12) mg/day for PCL10 during 1 month versus 0.02 mg/day delivered by eyedrops (Schmitz et al., 1999). The changes in IOP obtained in the eyes with implanted disk are similar to those obtained with the Ocusert drug delivery system (Macoul and Pavan-Langston, 1975). Trusopt® eyedrops produced the fastest decrease in IOP in normotensive eyes with peak IOP attained after 0.96 days, followed by blend disks in agreement with in vitro release results (peak IOP was reached fastest for blend disks with higher content of Lu). In hypertensive eyes, the same trend in IOP decrease was maintained, but the average IOP and peak IOP values were higher than those obtained in normotensive eyes. Peak IOP occurred at similar times in hypertensive eyes, except for Trusopt®. Probably, dorzolamide administered by eyedrops might require multiple doses to build up to steady state levels of concentration in the ciliary processes that are required for IOP decrease in hypertensive eyes.

3.5. Morphology and drug distribution, SEM and EPMA

SEM and EMPA were performed in order to determine the morphology of the disks and the drug distribution inside the disks before and after the in vivo implantation.

Fig. 3(a)–(f) shows the surface morphology of the prepared disks and in vivo degraded disks. There are significant signs of degradation on the implanted disk surface such as pores (Fig. 3(b)), cracks (Fig. 3(d)) and scales (Fig. 3(f)). The in vitro degraded samples showed fewer signs of material cracking (images not shown). This suggested enhanced degradation in vivo in comparison with in vitro conditions (see Section 3.6).

Table 6
Crystallinity, mass loss and molecular weight evolution for in vitro and in vivo degraded samples.

Sample	As prepared		In vitro		In vivo		M _w (g/mol)		ΔM _w (%)	
	X _{rel} (%)	-	X _{rel} (%)	Mass loss (%)	X _{rel} (%)	-	1 month		2 months	
							1 month	2 months	1 month	2 months
PCL40+drug	36.97 (1.93)	-	29.13 (0.97)	13.46 (1.14)	38.89 (0.03) ^a	-	62377.5 (725.5)	60274.5 (112.4)	4.9 ^b	8.1 ^b
PCL40	50.26 (0.33)	-	43.62 (1.27)	0.74 (0.11)	46.13 (1.62)	-	62727.3 (3555.6)	57653.5 (210.0)	4.4	12.1 ^b
PCL10+drug	40.06 (0.15)	-	42.26 (4.36)	22.68 (1.76)	50.66 (1.48)	-	16906.5 (2556.2)	-	10.8	-
PCL10	56.41 (0.34)	-	-	1.73 (0.42)	60.85 (1.51)	-	15152.5 (55.9)	-	0.7	-
6%Lu,PCL40+drug	32.12 (0.17)	-	38.51 (0.72)	36.77 (0.01)	47.18 (0.70) ^a	-	60625.5 (102.5)	-	7.6 ^b	-
6%Lu,PCL40	43.41 (0.19)	-	-	1.30 (0.10)	45.15 (1.79)	-	58144.5 (748.8)	-	11.4 ^b	-
13%Lu,PCL40+drug	30.32 (0.52)	-	41.43 (0.56)	41.12 (0.45)	44.07 (2.69)	-	61636.5 (2686.3)	-	6.0	-
13%Lu,PCL40	38.40 (1.13)	-	-	7.71 (0.56)	44.43 (2.96)	-	61606.0	-	6.1	-

^a $p < 0.05$ statistically significant differences relative to in vitro crystallinity.

^b $p < 0.05$ statistically significant differences relative to initial MW.

After preparation, the disks presented a heterogeneous drug distribution (Fig. 4(a)) probably because of phase separation between drug and polymers due to the high drug loading. After in vivo testing, there was almost no drug at the surface (Fig. 4(b)), while in the disk cross-section there were still significant amounts of drug present in sample PCL40 after 1 month in vivo (Fig. 4(c)). The mapping of the other disks sections show that the release was complete after 1 month of implantation.

3.6. In vitro and in vivo degradation

To differentiate between a physical or a chemical degradation mechanism, the crystallinity and MW was determined for initial, in vitro and in vivo degraded samples (Table 6 presents the change of disk crystallinity and MW due to in vitro and in vivo degradation). There was MW decrease due to chemical hydrolysis for PCL40+drug sample both after 1 month and 2 months and for 6%Lu,PCL40+drug after 1 month. Sample PCL10+drug did not degrade in vivo probably due to higher initial crystallinity as crystalline regions are more inaccessible to water uptake. The MW of the in vitro degraded samples was also determined, but the obtained differences were not statistically significant ($p \geq 0.17$). The samples presented lower crystallinity than the pure polymers (50.26 (0.33)% for PCL40 and 68.51 (2.12)% for Lu) and the drug loaded samples showed lower crystallinity than the control samples probably due to co-crystallization of dorzolamide (that is above the solubility limit in the polymer). In general, there was an increase in crystallinity for in vitro and in vivo degraded samples because the amorphous regions are degraded first and because during drug elution, the mobile polymer chains rearrange themselves and crystallize (Natu et al., 2010; Miyajima et al., 1997). Crystallinity was higher only for some in vivo degraded samples with respect to the in vitro degraded samples, suggesting that there is crystallinity increase and enhanced mechanical breakdown in vivo (see Section 3.7).

3.7. Histologic evaluation

The tissue samples collected from various organs showed normal cell morphology. The histological analysis of the tissues from the implantation site showed rapid resolution of the acute and chronic inflammatory stages and the development of normal foreign body reaction, consisting of adherent macrophages (Fig. 5(b)), fibroblasts, lymphocytes and foreign body giant cells (Fig. 5(c)) on the surface of the disk and fibrous capsule formation (Fig. 5(d)). Blood vessels (Fig. 5(a)) that formed in the fibrous capsule were also observed. There was a higher density of cells on the drug loaded disk with respect to control disks. No acute and/or chronic inflammation was seen after 2 months, indicating that the disks were biocompatible and did not produce inflammatory reactions characteristic to toxic materials.

4. Conclusions

Subconjunctival disks based on PCL and loaded with dorzolamide hydrochloride were implanted in rabbit eyes and their in vivo performance was assessed by their capacity to lower IOP in normotensive and hypertensive eyes. The high MW PCL showed non-cumulative release rates above the therapeutic level during 3 months. Histologic analysis showed normal foreign body reaction response consisting of adherent macrophages, fibroblasts, lymphocytes, foreign body giant cells and fibrous capsule formation. The release kinetics suggested a three stage release mechanism based on drug diffusion, polymer erosion and polymer degradation, with different steps depending on disk composition. In vivo, the fibrous

capsule formation around the PCL implant controls the drug release, working as a barrier membrane. For blend disks, due to polymer erosion that takes place mostly in the first day of release, the fibrous capsule/barrier control is absent.

In normotensive eyes, a 20% decrease in IOP obtained with the disks during 1 month was comparable with the one obtained by applying Trusopt® eyedrops. In hypertensive eyes, higher decrease percentages (around 40%) were obtained for all samples, with the most sustained decrease from the high MW PCL (40% after 1 month, 30% after 2 months). Peak IOP occurred earlier for blend disks due to enhanced drug release triggered by polymer erosion. It was proven that the devices can lower IOP in sustained manner in a rabbit glaucoma model. The blending offers the possibility to manipulate release rate and the amount of released drug in order to prepare devices tailored to the needs of patients (target IOP decrease percentages should take into account risk factors and disease progression).

Acknowledgements

The authors would like to thank Merck Sharp & Dohme Portugal for kindly supplying dorzolamide hydrochloride and Trusopt® eyedrops. FCT (Fundação para a Ciência e a Tecnologia) financial support is acknowledged by Mădălina V. Natu (SFRH/BD/30198/2006).

References

- Bourges, J.L., Bloquel, C., Thomas, A., Froussart, F., Bochot, A., Azan, F., Gurny, R., BenEzra, D., Behar-Cohen, F., 2006. Intraocular implants for extended drug delivery: therapeutic applications. *Adv. Drug. Deliv. Rev.*, doi:10.1016/j.addr.2006.07.026.
- Breitenbach, J., 2002. Melt extrusion: from process to drug delivery technology. *Eur. J. Pharm. Biopharm.* 54, 107–117.
- del Amo, E.M., Urtti, A., 2008. Current and future ophthalmic drug delivery systems A shift to the posterior segment. *Drug Discov. Today*, doi:10.1016/j.drudis.2007.11.002.
- Harris, A., Arend, O., Chung, H.S., Kagemann, L., Cantor, L., Martin, B., 2000. A comparative study of betaxolol and dorzolamide effect on ocular circulation in normal-tension glaucoma patients. *Ophthalmology* 107, 430–434.
- Khaw, P.T., Shah, P., Elkington, A.R., 2004. Glaucoma-2: treatment. *Br. Med. J.*, doi:10.1136/bmj.328.7432.156.
- Konstas, A.G., Kozobolis, V.P., Tsironi, S., Makridaki, I., Efremova, R., Stewart, W.C., 2008. Comparison of the 24-hour intraocular pressure-lowering effects of latanoprost and dorzolamide/timolol fixed combination after 2 and 6 months of treatment. *Ophthalmology*, doi:10.1016/j.ophtha.2007.03.007.
- Korte, J.M., Kaila, T., Saari, K.M., 2002. Systemic bioavailability and cardiopulmonary effects of 0.5% timolol eyedrops. *Graefes Arch. Clin. Exp. Ophthalmol.*, doi:10.1007/s00417-002-0462-2.
- Kulkarni, S.V., Damji, K.F., Buys, Y.M., 2008. Medical management of primary open-angle glaucoma: Best practices associated with enhanced patient compliance and persistency. *Patient Prefer. Adherence* 2, 303–313.
- Kuno, N., Fujii, S., 2010. Biodegradable intraocular therapies for retinal disorders: progress to date. *Drugs Aging* 27, 117–134, doi:10.2165/11530970-000000000-00000.
- Levkovitch-Verbin, H., Quigley, H.A., Martin, K.R.G., Valenta, D., Baumrind, L.A., Pease, M.E., 2002. Translimbal laser photocoagulation to the trabecular meshwork as a model of glaucoma in rats. *Invest. Ophthalmol. Vis. Sci.* 43, 402–410.
- Macoul, K.L., Pavan-Langston, D., 1975. Pilocarpine ocusert system for sustained control of ocular hypertension. *Arch. Ophthalmol.* 93, 587–590.
- Miyajima, M., Koshika, A., Okada, J., Ikeda, M., Nishimura, K., 1997. Effect of polymer crystallinity on papaverine release from poly(L-lactic acid) matrix. *J. Control. Release*, doi:10.1016/S0168-3659(97)00081-3.
- Nanjawade, B.K., Manvi, F.V., Manjappa, A.S., 2007. In situ-forming hydrogels for sustained ophthalmic drug delivery. *J. Control. Release*, doi:10.1016/j.jconrel.2007.07.009.
- Natu, M.V., Gil, M.H., de Sousa, H.C., 2008. Supercritical solvent impregnation of poly(ϵ -caprolactone)/poly(oxyethylene-*b*-oxypropylene-*b*-oxyethylene) and poly(ϵ -caprolactone)/poly(ethylene-vinyl acetate) blends for controlled release applications. *J. Supercrit. Fluids*, doi:10.1016/j.supflu.2008.05.006.
- Natu, M.V., de Sousa, H.C., Gil, M.H., 2010. Effects of drug solubility, state and loading on controlled release in bicomponent electrospun fibers. *Int. J. Pharm.*, doi:10.1016/j.ijpharm.2010.06.045.
- Natu, M.V., Gaspar, M.N., Ribeiro, C.A.F., Correia, I.J., Silva, D., de Sousa, H.C., Gil, M.H., 2011. A poly(ϵ -caprolactone) device for sustained release of an anti-glaucoma drug. *Biomed. Mater.* 6, 025003, doi:10.1088/1748-6041/6/2/025003.
- Noecker, R.J., 2005. Evaluation of bimatoprost 0.03% versus latanoprost 0.005%: a paired comparison study. *Invest. Ophthalmol. Vis. Sci.* 46, E-Abstract 2452.
- Pitt, C.G., Chasalow, F.I., Hibionada, Y.M., Klimas, D.M., Schindler, A., 1981. Aliphatic polyesters. I. The degradation of poly(ϵ -caprolactone) in vivo. *J. Appl. Polym. Sci.*, doi:10.1002/app.1981.070261124.
- Quigley, H.A., 2005. Glaucoma: macrocosm to microcosm. *Invest. Ophthalmol. Vis. Sci.*, doi:10.1167/iovs.041070.
- Ruiz-Ederra, J., Verkman, A.S., 2006. Mouse model of sustained elevation in intraocular pressure produced by episcleral vein occlusion. *Exp. Eye Res.*, doi:10.1016/j.exer.2005.10.019.
- Schmitz, K., Banditt, P., Motschmann, M., Meyer, F.P., Behrens-Baumann, W., 1999. Population pharmacokinetics of 2% topical dorzolamide in the aqueous humor of humans. *Invest. Ophthalmol. Vis. Sci.* 40, 1621–1624.
- Schwartz, K., Budenz, D., 2004. Current management of glaucoma. *Curr. Opin. Ophthalmol.* 15, 119–126.
- Scozzafava, A., Menabuoni, L., Mincione, F., Briganti, F., Mincione, G., Supuran, C.T., 1999. Carbonic anhydrase inhibitors. synthesis of water-soluble, topically effective, intraocular pressure-lowering aromatic/heterocyclic sulfonamides containing cationic or anionic moieties: is the tail more important than the ring? *J. Med. Chem.*, doi:10.1021/jm9900523.
- Seki, M., Tanaka, T., Matsuda, H., Togano, T., Hashimoto, K., Ueda, J., Fukuchi, T., Abe, H., 2005. Topically administered timolol and dorzolamide reduce intraocular pressure and protect retinal ganglion cells in a rat experimental glaucoma model. *Br. J. Ophthalmol.*, doi:10.1136/bjo.2004.052860.
- Yasukawa, T., Ogura, Y., Sakurai, E., Tabata, Y., Kimura, H., 2005. Intraocular sustained drug delivery using implantable polymeric devices. *Adv. Drug Deliv. Rev.* 57, 2033–2046, doi:10.1016/j.addr.2005.09.005.
- Yudcovitch, L. Pharmaceutical, laser and surgical treatments for glaucoma: an update. <http://www.pacificu.edu/optometry/ce/courses/15166/pharglap2.cfm#Pharmaceutical> (accessed 15.10.10).